

1  
2 **EFFECT OF KINEMATIC INTERACTION ON SEISMIC RESPONSE OF**  
3 **OFFSHORE WIND TURBINES ON MONOPILES**

4  
5 **Amir M. Kaynia<sup>1,2</sup>**  
6

7 <sup>1</sup>Norwegian Geotechnical Institute (NGI), Oslo, Norway  
8

9 <sup>2</sup>Norwegian University of Science and Technology (NTNU), Trondheim, Norway  
10

11 Interest in renewable energy over the past decade has motivated a remarkable research on offshore wind energy.  
12 Due to the environmental loading conditions in the early developments of offshore wind farms, the focus of the  
13 research and engineering has been on aerodynamic and hydrodynamic subjects. However, earthquake has turned  
14 out to be a major design concern in seismic areas such as East Asia, Southern Europe and United states. The topics  
15 include, among others, nonlinear response of foundations, soil liquefaction and their impacts on foundation  
16 performance. An important topic in seismic soil-structure interaction (SSI) analysis is the kinematic seismic  
17 response of foundations. This information is crucial for analyses based on the sub-structuring approach where both  
18 kinematic response and foundation impedances are key parameters. While considerable research has been spent  
19 on the latter topic, very little has been reported on the kinematic interaction. Large monopoles with low aspect  
20 ratios tend to rotate much more than regular piles in pile group foundations due to seismic waves. The rotation  
21 leads to additional load on the tower and the turbine. This paper uses a rigorous numerical model for monopole-  
22 soil interaction in layered soil and computes both rotational and horizontal responses at the pile head (seabed) as  
23 functions of frequency. A suite of generic homogeneous and heterogeneous soil profiles with shear moduli  
24 representative of clay (generally linear) and sand (generally parabolic) are considered in these analyses. Through  
25 representative analyses, both in frequency domain and time domain, it is illustrated how the kinematic interaction  
26 influences the earthquake loads imparted to an offshore wind turbine (OWT).  
27

28 **KEYWORDS**  
29

30 Wind turbine; Earthquake response; Soil-structure interaction; Kinematic interaction; Seismic performance  
31

32 **INTRODUCTION**  
33

34 Earthquake response of piles has been studied extensively over the past five decades. The developments in the  
35 nuclear power industry in the 1960s and 1970s was a major driving force in this field especially in computation of  
36 the impedances of pile groups, while use of piles for onshore and offshore structures has focused on their design  
37 under earthquake loading with or without liquefaction. Most of the performed research have been related to the  
38 inertial interaction of pile foundations. The kinematic interaction studies have mostly focused on the forces in the  
39 piles. This is partly due to the observation that pile foundations, which are often connected to rigid pile caps, follow  
40 the ground motions (e.g. Kaynia, 1982; Fan et al., 1991; Miura et al., 1994). The studies on kinematic internal  
41 forces have ranged from simple engineering solutions (e.g. Dobry and O'Rourke, 1983; Pender, 1993; Mylonakis  
42 et al., 1997; Nikolaou et al. 2001; Mylonakis, 2001; Di Laora and Rovithis, 2015; Dezi et al., 2016;) to numerical  
43 FE-based methods (e.g. Boulanger et al., 1999; Varun et al., 2008; Maiorano et al., 2009) and to rigorous  
44 elastodynamics solutions (e.g. Kaynia and Mahzooni, 1996; Waas and Hartmann, 1984; Kaynia and Novak, 1992;  
45 Padron et al. 2008). A few studies have separately considered the effect of pile diameter on the kinematic  
46 interaction forces (e.g. Di Laora et al. 2017). More recently, advanced constitutive models (e.g. Manzari and  
47 Dafalias, 1997; Elgamal et al, 2002; Dafalias and Manzari, 2004; Andrianopoulos et al. 2010) have been used for  
48 response of different types of piles in liquefiable soil (Kementzetzidis et al. 2019; Esfeh and Kaynia, 2020).  
49

50 Interest in renewable energy in the past decade has motivated a remarkable research on offshore wind energy. Due  
51 to the environmental loading conditions in the early developments of offshore wind farms, the focus of the research  
52 and engineering has been on aerodynamic and hydrodynamic subjects. However, earthquake has turned out to be  
53 a major design concern in seismic areas such as East Asia, Southern Europe and United states. The topics include,  
54 among others, nonlinear response of foundations and soil liquefaction and their impact on foundation performance

1 (Kaynia, 2019). The available computational models have been applied or extended to the dynamic analysis of  
2 monopiles in offshore wind turbines in the past several years (e.g. Kourkoulis, 2014; Kjølraug and Kaynia, 2015;  
3 Bayat et al. 2016; Shadlou and Bhattacharya, 2016; Álamo et al., 2018; Markou and Kaynia 2018; He et al. 2019;  
4 Auersch, 2019). Monopiles are characterized by large diameter steel pipe sections (diameters ranging from 5 m to  
5 10 m) and relatively short length. With such dimensions, the monopiles approach embedded caissons which are  
6 expected to undergo considerable rotation due to the kinematic interaction during earthquake shaking. The rotation  
7 leads to additional displacements in the tower and higher loads in the tower and the turbine. While considerable  
8 research has been spent on the impedances of large monopiles, very little has been reported on their kinematic  
9 interaction response. This issue is addressed in this paper which uses a rigorous numerical model for monopile-  
10 soil interaction in layered soil and computes both rotational and horizontal responses at the pile head (seabed level)  
11 as functions of frequency. A range of generic homogeneous and heterogeneous soil profiles with shear moduli  
12 representative of clay (generally linear) and sand (generally parabolic) is considered. Through analyses of a  
13 representative offshore wind turbine (OWT) model, it is illustrated how the kinematic interaction influences the  
14 earthquake loads imparted to OWTs.

15  
16 The computational model used in the present study is PILES (Kaynia, 1982). The pile-soil tractions in this model  
17 are replaced by piecewise constant cylindrical loads on the pile shaft and circular load at the pile tip. By using  
18 analytically derived Green's functions for these loads in layered soil media, a soil stiffness matrix is established  
19 and is coupled to the dynamic stiffness matrix of the monopile. The response of the monopile is then computed by  
20 imposition of the relevant boundary and traction conditions. The analyses are carried out under steady-state  
21 harmonic vibration in the frequency domain. The results of analyses, such as impedances and seismic motions, are  
22 therefore complex-valued quantities. Representative time history responses are computed using the Fourier  
23 Transform technique. The seismic excitation is assumed to be due to vertically shear waves. For details of the  
24 model see Kaynia (1982) and Kaynia and Kausel (1991).

## 26 **PARAMETERS OF SOIL PROFILES AND OWT MODEL**

### 28 **OWT Model**

29  
30 For the OWT model the NREL 5-MW offshore baseline wind turbine, symbolically presented in Figure 1, was  
31 used. This is a reference offshore wind turbine defined by National Renewable Energy Laboratory (Jonkman et al.  
32 2009) for researchers to use as a common reference model in their studies. This reference model is a three-bladed  
33 upwind horizontal axis wind turbine (HAWT) with a monopile support structure. The data for this wind turbine is  
34 summarized in Table 1. The first and second natural frequencies of the tower on rigid base are respectively 0.32  
35 Hz and 2.9 Hz in the fore-aft direction (normal to blades) and 0.31 and 2.94 Hz in the side-side direction. As shown  
36 by the results presented in this paper, the natural frequencies are reduced due to the foundation flexibility  
37 depending on soil stiffness. Figure 1 also indicates the positive direction of horizontal displacements and rotations  
38 of the structure.

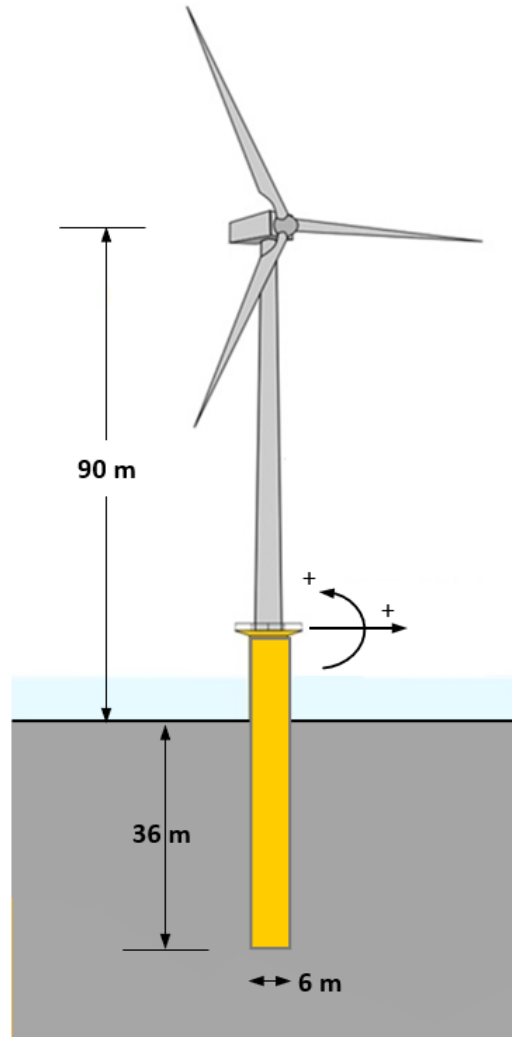
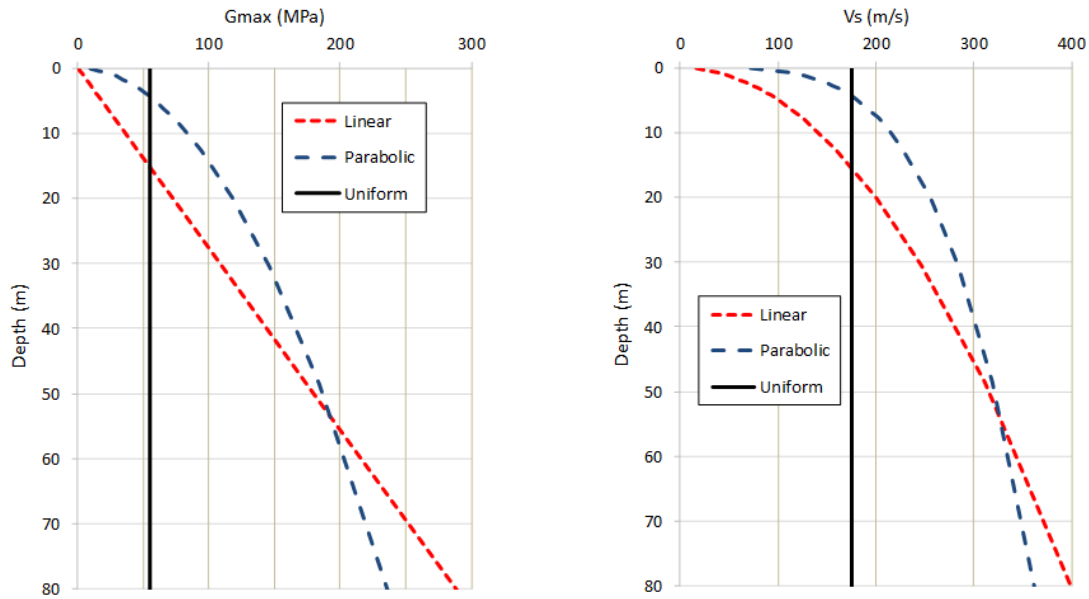


Figure 1 – Schematics of OWT reference model used in present study

### Soil Profiles

Three soil profiles were considered in the analyses as follows: a) Uniform (homogeneous) soil profile with a constant shear wave velocity of  $V_s = 175$  m/s corresponding approximately to the reference soil profile considered in several studies using NREL model (e.g. Løken and Kaynia, 2019), b) Parabolic variation of shear modulus, representing typical sandy sites, and c) Linear variation of shear modulus, representing typical saturated normal-consolidated clays. The small-strain shear modulus,  $G_{max}$ , for the linear (clayey) profile was taken as 1500 times the assumed shear strength of the soil varying with depth equal to  $0.30 \sigma'_v$  where  $\sigma'_v$  is the effective vertical stress. For the parabolic (sandy) profile,  $G_{max}$  was computed using the empirical formula by Seed and Idriss (1970) for sand with relative density  $D_r = 60\%$ . Using the suggested parameter by Seed and Idriss (1970), one can establish the formula  $G_{max} = 1140 (p_a \sigma'_m)^{0.5}$  where  $p_a = 100$  kPa is the atmospheric pressure, and  $\sigma'_m$  is the average effective confining stress.

Figure 2 displays these profiles both in terms of shear modulus and shear wave velocity. In addition, the unit soil mass, Poisson's ratio and damping ratio in all three profiles were taken as  $1800$  kg/m<sup>3</sup>,  $0.4$  and  $0.05$ , respectively. The selected damping is a reference value used in all the analyses and is not meant to correspond to a specific shear strain as it is common to consider in nonlinear soil dynamic analyses. The profiles are displayed down to  $80$  m in Figure 2. Below this depth the soil is assumed to be uniform with the soil parameters at  $80$  m.



1  
2 **Figure 2 – Soil profiles considered in this study in terms of variation with depth of shear modulus (left)**  
3 **and shear wave velocity (right).**  
4

5 **COMPUTATIONAL MODEL AND ANALYSIS CASES**  
6

7 The analyses were carried out for shear waves propagating vertically and generating a unit horizontal acceleration  
8 on the soil surface (seabed) in the free field. The tower structure was modelled by twelve beam elements with  
9 variable bending rigidity and mass corresponding to a linear variation of tower diameter and wall thickness in  
10 accordance with Table 1. The bending rigidity in the transition piece (bottom 15 m of the tower over seabed shown  
11 in Fig. 1) was slightly increased to obtain a better match with the natural frequencies of NREL model. The hub  
12 and nacelle were modelled together as a lumped mass at the top node of the tower's FE model.  
13

14 The monopile was represented by a  $2 \times 2$  complex-valued impedance matrix, computed by PILES, representing the  
15 relationship between the horizontal force and bending moment at the top of the monopile and the associated  
16 displacement and rotation. This impedance matrix is assembled to the dynamic stiffness matrix of the tower.  
17 Because PILES solves the governing dynamic equations in each soil layer analytically, there is no restrictions for  
18 selection of layer thicknesses. However, the thicknesses should be selected to capture the general shape of the  
19 deformed pile. For the present study, between 17 to 21 soil layers (depending on the pile length) were selected  
20 with thicknesses varying from 0.25 m at the pile head to about 5 m at the pile tip.  
21

22 **Table 1 - Properties of NREL 5-MW baseline wind turbine (Jonkman et al. 2009)**  
23

Property	Value
Rating	5 MW
Rotor orientation, configuration	Upwind, 3 blades
Rotor diameter, hub diameter	126 m, 3 m
Hub height	90 m
Cut-in, rated, cut-out wind speed	3, 11.4, 25 m/s
Rated rotor speed	12.1 rpm
Rated tip speed	80 m/s
Rotor mass	110 000 kg
Nacelle mass	240 000 kg
Tower mass	347 466 kg
Tower top diameter, wall thickness	3.87 m, 0.019m
Tower base diameter, wall thickness	6 m, 0.027 m
Substructure base diameter, wall thickness	6 m, 0.06 m

1

2 If the nodes of the tower are denoted by  $T$  and those at the tower-pile interface (pile head) by  $P$ , then the matrix  
3 equation of tower-pile inertial interaction can be written as (e.g. Kausel et al., 1978)

4

$$5 \begin{bmatrix} K_{TT} & K_{TP} \\ K_{PT} & K_{PP} + X_P \end{bmatrix} \begin{Bmatrix} U_T \\ U_P \end{Bmatrix} = \begin{Bmatrix} 0 \\ X_P U^* \end{Bmatrix} \quad (1)$$

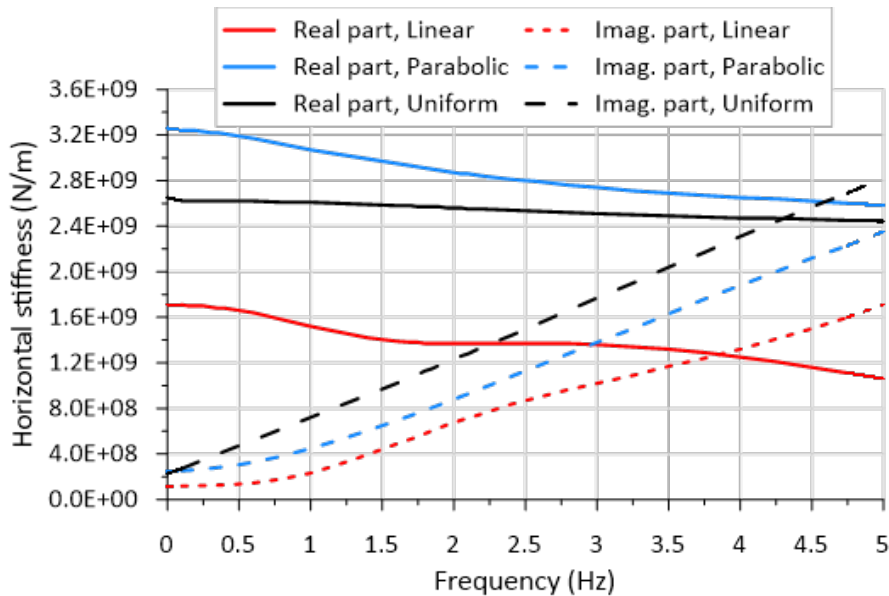
6

7 where  $K_{TT}$ ,  $K_{PP}$  and  $K_{TP}$  denote the parts of the tower's stiffness matrix corresponding to the nodes  $T$ ,  $P$  and their  
8 coupling, respectively,  $X_P$  represents the  $2 \times 2$  impedance matrix of the monopile, and  $U^*$  represents the  $2 \times 1$  vector  
9 of kinematic interaction displacement and rotation at monopile head (that is, the displacement and rotation of the  
10 monopile head due to the seismic waves in the absence of the tower). The vectors  $U_T$  and  $U_P$  are the vectors of  
11 displacements and rotations of the FE nodes of the tower ( $T$ ) and pile head ( $P$ ). The positive directions of horizontal  
12 displacement and rotation are indicated in Figure 1.

13

14 Figure 3 plots the variation with frequency of the real and imaginary parts of the horizontal impedance of the  
15 monopile (i.e. entry  $X_{11}$  in the foundation impedance matrix) for the three soil profiles considered in this study. As  
16 well known, the real part represents the combined effect of static stiffness and added soil mass, and the imaginary  
17 part represents the combined values of hysteretic and radiation damping. The figure shows that the horizontal  
18 stiffness and damping of the linear soil profile (clay) is considerably smaller than those of the other two soil  
19 profiles.

20



21

22 **Figure 3 – Horizontal impedance of monopile in three soil profiles**

23

24 Figure 4 displays the corresponding results for the rocking stiffness (entry  $X_{22}$  in the foundation impedance matrix).  
25 It is interesting to note that the rocking stiffness are relatively similar in the three soil profiles.

26

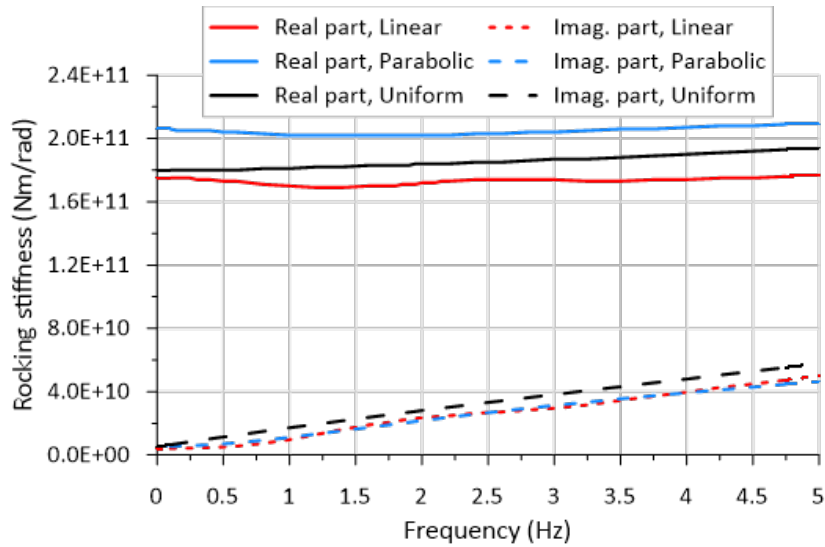


Figure 4 – Rocking impedance of monopile in three soil profiles

Figure 5 displays the absolute values of the kinematic interaction responses of the monopile in the three soil profiles (the entries of the vector  $U^*$ ). Figure 5(a) shows the horizontal displacement normalized by the free-field seabed displacement, and Figure 5(b) shows the corresponding rotation, again normalized in value by the horizontal free-field displacement. The figures show a clear difference in kinematic response of the monopile in the linear soil profile compared to the other profiles. As the plots in Figure 5 show, while the pile head displacement is larger than the seabed displacement for frequencies in the range about 1-3 Hz in the Uniform and Parabolic soil profiles, it is considerably smaller than the seabed displacement for all frequencies in the Linear soil profile. This issue has consequence for the dynamic response of the OWT which is discussed in the next section.

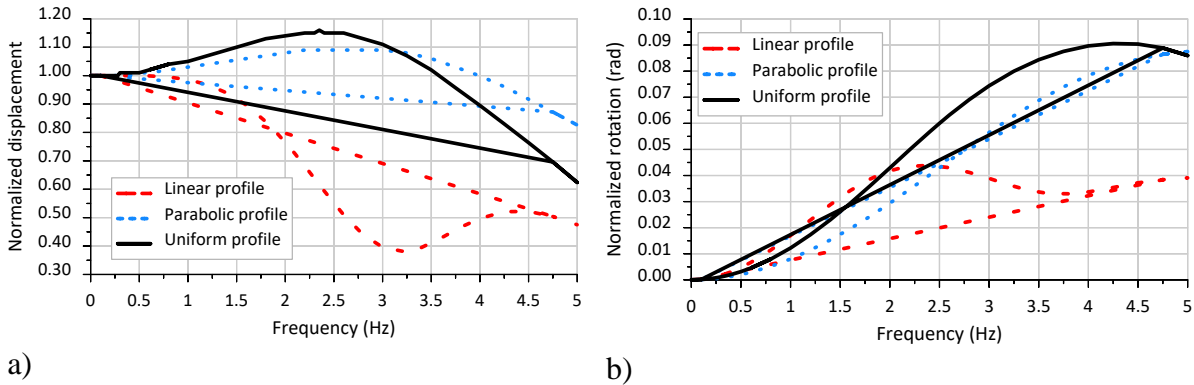


Figure 5 – Absolute values of kinematic interaction response of monopile in three soil profiles, a) normalized horizontal displacement of pile head, b) normalized rotation of pile head

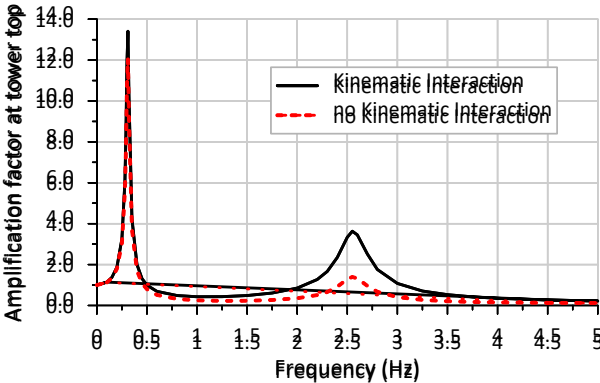
## ANALYSES AND RESULTS

This section presents representative results for the inertial interaction response of the complete system in the frequency domain. Representative time history results are presented in the next section. The results in this section include variation with frequency of the displacement/acceleration at the top of tower (hub/nacelle) and bending moment at the base of tower. All the results are presented in normalized form. The displacement/acceleration of the tower top is normalized by the free-field seabed displacement/acceleration. The analyses are for visco-elastic pile-soil response; therefore, the actual seabed displacement/acceleration have no effect when the results are presented in normalized form. The frequencies, on the other hand are shown in real (non-dimensional) values. This allows easier comparison between the cases and better connection between the results and the characteristics of real earthquake shakings.

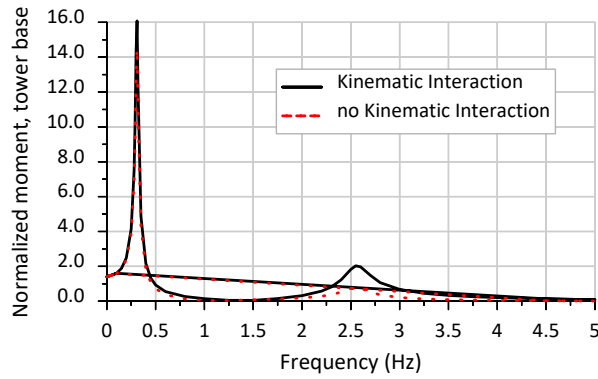
1 To highlight the importance of kinematic interaction two sets of analyses were performed. In the first set, the  
 2 complete SSI analyses including kinematic interaction was performed according to Eq. 1. In the second set, the  
 3 kinematic interaction was ignored by setting the horizontal pile head motion equal to the seabed motion and  
 4 ignoring the pile head rotation; that is, the first entry in the vector  $U^*$  was set to 1.0 for all frequencies and the  
 5 second element was taken equal to zero. This case represents the analysis in which the seabed ground motion is  
 6 directly used for excitation of the tower. This is the assumption in the analysis of most structures on pile  
 7 foundations. It is important to note that for the sake of consistency the same foundation impedance was used in  
 8 both analyses. The results and conclusions might change if a different foundation impedance is used in the case  
 9 with no kinematic interaction, for example, if the cross-coupling term in the  $2 \times 2$  impedance matrix of the monopile  
 10 is ignored (as is sometimes done for simplicity) and the foundation is represented by just the diagonal terms of the  
 11 impedance matrix (i.e. uncoupled horizontal and rotational springs).  
 12

13  
 14 Figure 6 presents the variation with frequency of the amplification of motions at the tower top relative to the free-  
 15 field surface ground motion in the Uniform soil for the two analyses, namely, with and without kinematic  
 16 interaction. The peaks correspond to the first and second natural frequencies of the SSI system which are about  
 17 0.3 and 2.55 Hz. Due to SSI, the natural frequencies are lower than the natural frequencies of the tower on fixed  
 18 base (i.e. 0.31 and 2.9 Hz). Note that due to the foundation damping, the mode shapes are complex-valued vectors  
 19 with real and imaginary parts. The forms of both parts are generally similar to the bending mode shapes of a  
 20 cantilever beam representing the tower. The results in this figure show practically identical responses except at  
 21 frequencies around the second mode which indicate that kinematic interaction will have non-negligible effect if  
 22 the excitation has medium-to-high frequency components (e.g. 1-3 Hz).  
 23

24 For the same soil profile, Figure 7 displays the variation with frequency of the normalized bending moment at the  
 25 tower base for the two sets of analyses. The normalization is with respect to the moment generated by the lumped  
 26 mass of rotors/nacelle on tower top ( $m_T = 350$  tons, Table 1) shaken by the free-field ground acceleration,  $a_g$ ; that  
 27 is,  $m_T a_g H$  where  $H = 90$  m is the height of the tower (Fig. 1 and table 1). For the selected motions with  $a_g = 1$  m/s<sup>2</sup>  
 28 on ground surface the normalization factor is  $3.15 \times 10^7$  Nm. The conclusion on the role of kinematic interaction is  
 29 practically the same. The significance of the above observation and the role of earthquake's frequency  
 30 characteristics are demonstrated in the next section through time history analyses of real earthquake records.  
 31



32  
 33 **Figure 6 – Amplification of ground motion on top of tower in Uniform soil profile. Results are normalized**  
 34 **with free-field seabed motions for cases including kinematic interaction and excluding kinematic**  
 35 **interaction**  
 36  
 37



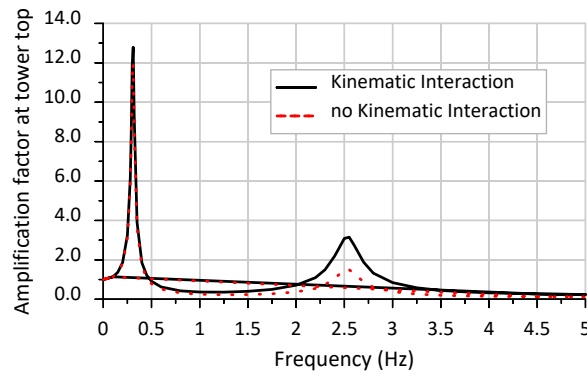
1

2 **Figure 7 – Normalized bending moment at base of tower in Uniform soil profile. Results are normalized**  
 3 **with moment generated by the lumped mass (nacelle/rotors) at tower top excited by free-field ground**  
 4 **acceleration ( $1 \text{ m/s}^2$ ).**

5

6 Figures 8 and 9 present the same set of results (tower top motion and tower base moment, respectively) for the  
 7 Parabolic (sandy) soil profile. The observations about the response amplifications in the case with kinematic  
 8 interaction for the medium-to-high frequency range are similar to those made above for the Uniform profile.

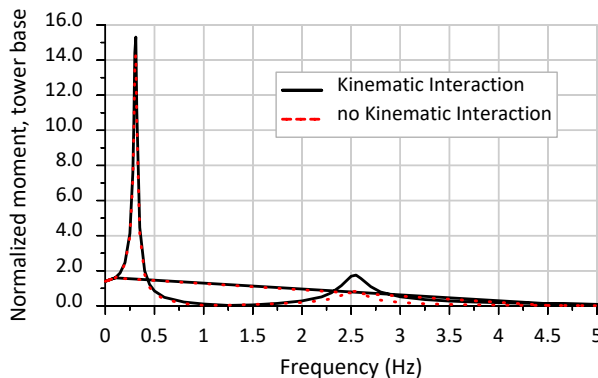
9



10

11 **Figure 8 – Amplification of ground motion on top of tower in parabolic soil profile for cases including**  
 12 **kinematic interaction and excluding kinematic interaction.**

13



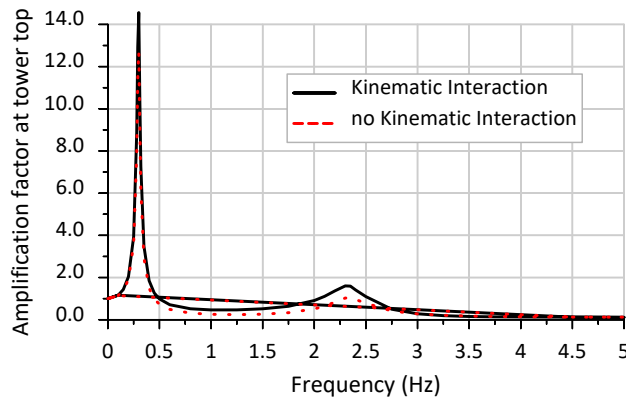
14

15 **Figure 9 – Normalized bending moment at base of tower in Parabolic soil profile for cases including**  
 16 **kinematic interaction and excluding kinematic interaction.**

17



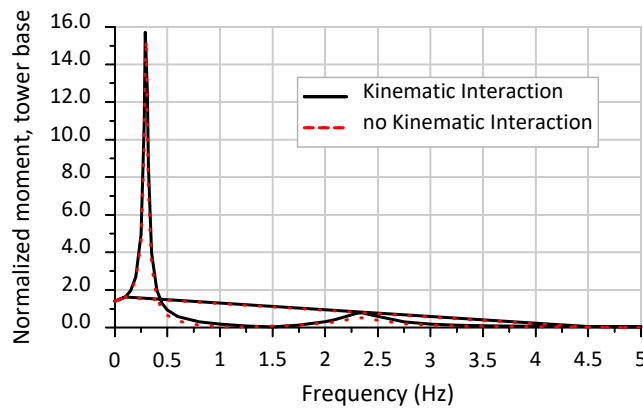
1 The results are slightly different for the Linear soil profile. Figure 10 presents the amplification of motions with  
2 frequency at the tower top for the Linear soil profile. Firstly, the figure indicates a lower natural frequency for the  
3 Linear profile compared with the Uniform and Parabolic profiles (for example, natural frequency of the second  
4 mode is about 2.35 Hz vs. 2.55 Hz in the other two profiles). This is due to the lower stiffness of the monopile in  
5 the Linear profile. However, it might seem surprising that a reduction of the pile stiffness by about 50% has resulted  
6 in only 10% reduction of the natural frequencies. This is partly because natural frequency is proportional to square  
7 root of stiffness and partly because the overall SSI stiffness is dominated by the pile stiffness, therefore, 50%  
8 reduction of the pile stiffness leads to less reduction in the system's stiffness. Secondly, the amplitude of response  
9 amplification at the second natural frequency seems less than the corresponding amplifications in the other two  
10 profiles. This can probably be explained by the smaller kinematic pile-head displacement at this frequency (see  
11 Fig. 3). The variation of the normalized bending moment with frequency is displayed in Figure 11.  
12



13

14 **Figure 10 – Amplification of ground motion on top of tower in Linear soil profile for cases including and**  
15 **excluding kinematic interaction.**

16



17

18 **Figure 11 – Normalized bending moment at base of tower in Linear soil profile for cases including and**  
19 **excluding kinematic interaction.**

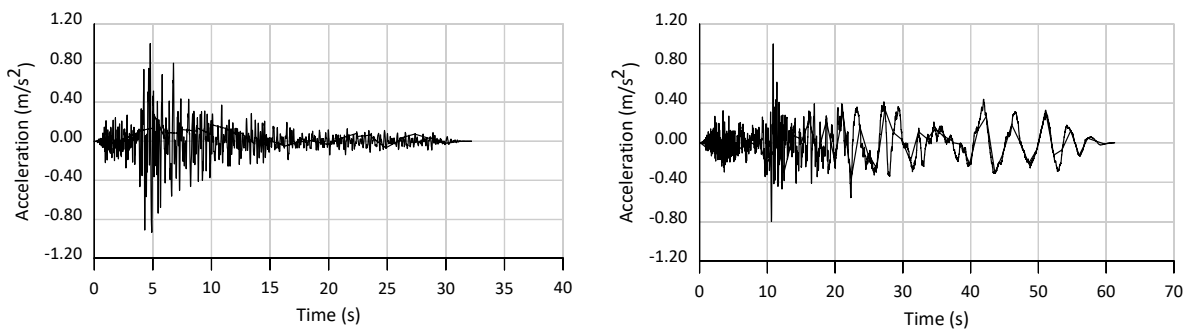
20

21 The above results could have a significant implication for design. They reveal that exclusion of the kinematic  
22 interaction might have a significant impact on the tower response and internal forces, and this depends on the  
23 frequency characteristics of the earthquake shaking. This is investigated through time history analyses in the next  
24 section.  
25  
26  
27  
28

1 ANALYSES IN TIME DOMAIN

2

3 To better capture the effect of higher frequencies on the seismic response of OWTs two earthquake time  
4 histories with distinctly different frequency characteristics were considered and the responses of the  
5 OWT in the Parabolic profile, with and without kinematic interaction effect, were computed. The  
6 records were selected from the PEER strong motion database (<https://peer.berkeley.edu/peer-strong-ground-motion-databases>). They are Whittier Narrows-01, Beverly Hills - 12520, dated 10/1/1987, and  
7 Chi-Chi Taiwan-03, CHY082, dated 9/20/1999. These acceleration time histories are normalized to  
8  $PGA = 1 \text{ m/s}^2$  and are plotted in Fig. 12 together with their response spectra presented in Figure 13.  
9 These acceleration records are assumed to be the free-field motions on the ground surface. The response  
10 spectra show that while the Whittier Narrows record is rich in high frequencies, ChiChi is strongly  
11 characterized by low frequencies. In view of the results presented in the previous section, one would  
12 then expect that the seismic response of the OWT due to ChiChi will be affected only marginally by the  
13 kinematic interaction, while it will be strongly affected by Whittier Narrows.  
14  
15  
16

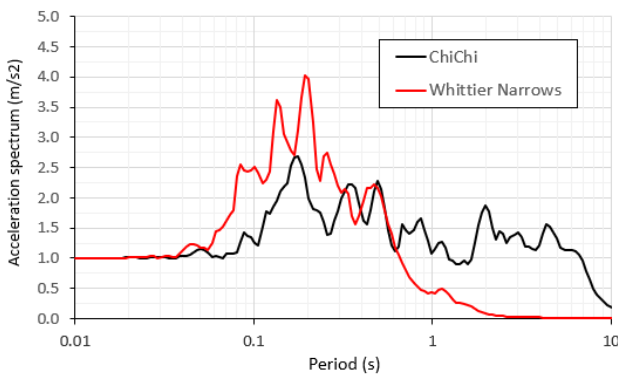


17

18 **Figure 12 – Acceleration time histories of Whittier Narrows (left) and ChiChi (right) normalized to  $PGA = 1 \text{ m/s}^2$**

19

20



21

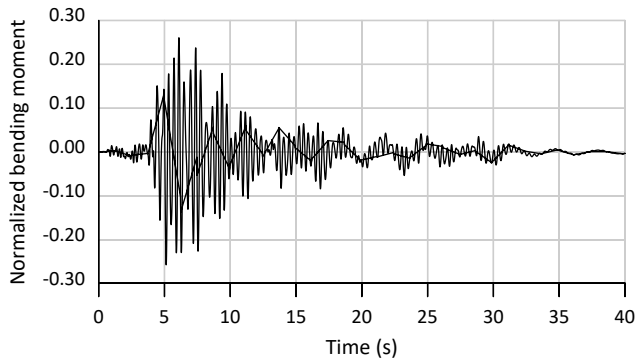
22

23 **Figure 13 – Response spectra for acceleration time histories in Figure 12.**

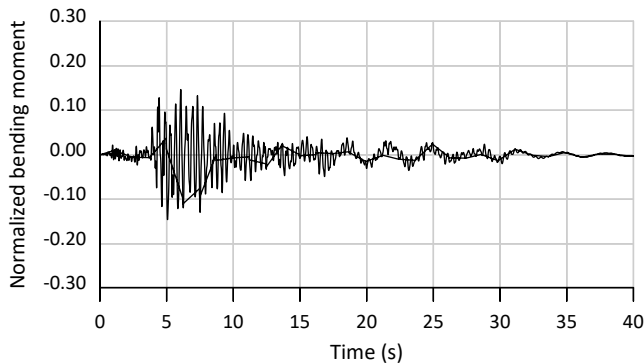
24

25

26 Figure 14 plots the time histories of the computed normalized bending moment at the tower base due to  
27 Whittier Narrows for both kinematic interaction (Fig. 14a) and no kinematic interaction (Fig. 14b) (note  
28 normalization of bending moment with  $m_T a_g H$  as introduced above). This record is rich in high  
29 frequencies, and as expected it has created a larger response in the model when kinematic interaction is  
30 included. The ratio between the peak bending moments is about the same as the ratio of the peaks at the  
31 second natural frequency in Fig. 9. Careful examination of Fig. 14a reveals that the response is  
32 dominated by the oscillations with frequency 2.5 Hz due to the second mode superimposed on a weaker  
33 response from the first mode at frequency 0.3 Hz.  
34



(a)

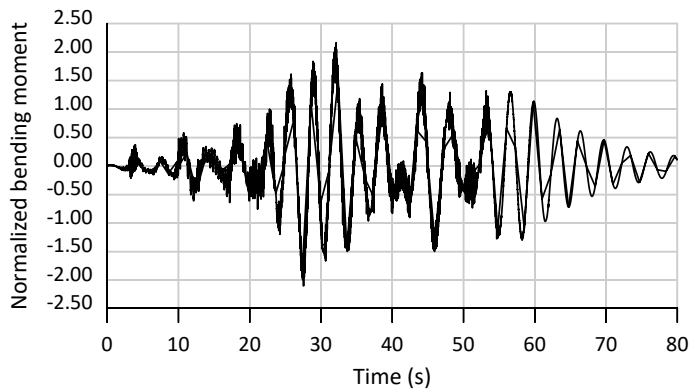


(b)

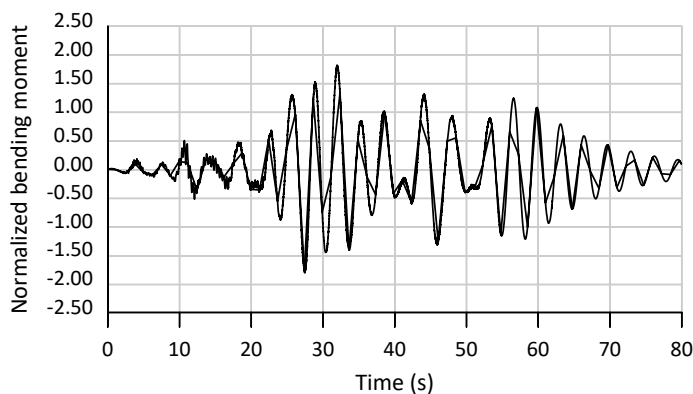
**Figure 14 – Time histories of normalized bending moment at base of tower due to Whittier Narrows time history for cases a) including kinematic interaction, and b) excluding kinematic interaction.**

A different form of response is obtained when the OWT is subjected to ChiChi record. Figure 15 displays the computed normalized bending moments at the base of the OWT (with and kinematic interaction) for this earthquake record. Both plots in this figure show that the response is dominated by the first mode although one can clearly see a trace of the second mode response. It is interesting to note that the influence of the second mode is again higher in the case with kinematic interaction, especially in the early phase of shaking where the record has a stronger presence of high frequencies.

The clear conclusion from the above results is that kinematic interaction has a relatively large effect on the response of OWTs and should be carefully incorporated especially if the excitation is characterized by frequencies in the mid-to-large range. The key issue is if the second mode lies in this range.



(a)



(b)

**Figure 15 – Time histories of normalized bending moment at base of tower due to ChiChi time history for cases a) including kinematic interaction, and b) excluding kinematic interaction.**

## PRACTICAL CONSIDERATIONS

The above analyses and results have clearly highlighted the importance of inclusion of kinematic interaction in the seismic analyses of OWTs. From a practical point of view, there are several issues that have bearing on this discussion. Two of them, namely the soil nonlinearity and sensitivity of the results to pile-soil parameters, are studied in the following.

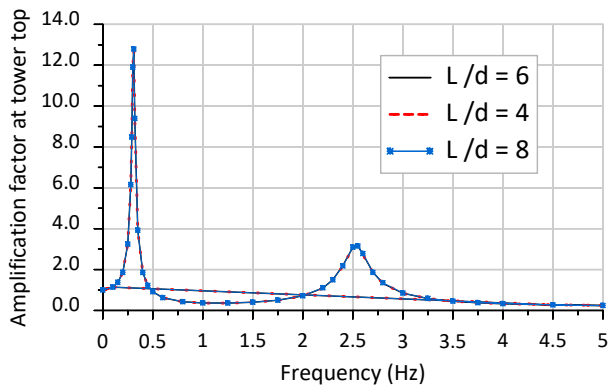
### Effect of soil nonlinearity

The analyses and results presented in this study have assumed a visco-elastic soil response. Obviously, for earthquake shaking to be a governing design load case, the shaking should be relatively strong which would cause soil nonlinearity in most soil sites. The common practice in such cases is to perform site response analyses and use the strain-compatible modulus and damping values in the SSI analyses without accounting for secondary nonlinearity due to pile-soil interaction. Following this approach, one would often end up with modified design soil profiles with shear moduli reduced typically between 20% and 50% (corresponding reduction in shear wave velocity 10-30%). The reduction is potentially more in soft soils (such as the Linear profile considered in this study) due to strong shaking. Considering the trend of the results presented in this study for different soil profiles (for example results for the stiff Parabolic profile vs. those for the soft Linear profile), one could qualitatively conclude that soil nonlinearity tends to reduce the effect of kinematic interaction, due to both change in the frequency characteristics of the shaking and the reduced role of the second mode.

1 Sensitivity to pile-soil parameters

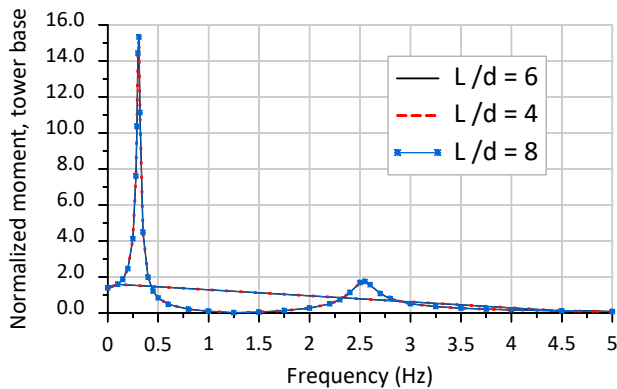
2 The analyses presented in this study were carried out for a typical monopile design and a limited  
3 number of soil profiles but with realistic parameters. There are several soil parameters that could  
4 influence the established shear wave velocity profiles; however, it is believed that the selected profiles  
5 practically cover the range of soil parameters encountered in practice. Moreover, the results are  
6 consistent in terms of the response mechanism, role of the second structural mode and the role of  
7 kinematic interaction. Therefore, no attempt was made in this study to expand the range of soil  
8 profiles. On the other hand, the length of the monopile might be considered an important parameter as  
9 it influences the rotation of the foundation. Therefore, a limited sensitivity analysis was performed by  
10 varying the pile length-diameter ratio  $L/d$  from 4 to 8 in the parabolic soil profile. The monopile used  
11 in the previous sections has  $L/d = 6$ . Recent studies (e.g. Løken and Kaynia, 2019), have indicated that  
12 earlier monopile designs (and even recently in many cases) have been on the conservative side, and  
13 lower pile lengths could be satisfactory, for example as low as  $L/d = 4$ .

14 Figure 16a displays the variation with frequency of the amplification of ground motion on top of the  
15 tower for the three  $L/d$  cases 4, 6 and 8, and Figure 16b shows the corresponding normalized bending  
16 moment at the tower base. The plots in these figures indicate no sensitivity to the pile length in the  
17 range considered. The kinematic interaction responses (as in Fig. 5) show practically the same  
18 variations for the three  $L/d$  cases (results not shown for brevity). This result is related to the ratio  
19 between the pile length and the wavelength in the soil and is therefore not general. However, from the  
20 cases considered here (as well a similar assessment for the Linear profile not shown here), this  
21 parameter does not appear to be a governing parameter for the ranges of soil profiles and pile  
22 dimensions encountered in practice.



23

24 a)



25

26 b)

27 **Figure 16 – Effect of pile length to diameter ratio on seismic response of OWT in Parabolic soil, a)**  
28 **amplification of ground motion on top of tower, b) normalized bending moment at base of tower.**

1  
2  
3 **SUMMARY AND CONCLUSIONS**  
4

5 This paper used a rigorous numerical model for monopole-soil interaction in layered soil and computed both  
6 rotational and horizontal kinematic responses at the monopile head (seabed level) as functions of frequency. The  
7 intention was to assess if one could ignore the kinematic interaction and simply use the free-field horizontal seabed  
8 motion as the input to the tower's response. Three soil profiles with variations of shear modulus representing  
9 uniform, sandy and clayey sites were considered. Two sets of analyses were carried out. In the first set, the  
10 complete SSI analysis, including kinematic interaction, was performed, and in the second set, the kinematic  
11 interaction was ignored by directly using only the horizontal seabed motion as the excitation of the tower. The  
12 analyses have led to the following conclusions.

13  
14 a) In all the soil profiles considered, the tower response and bending moments are larger when kinematic  
15 interaction is included in the SSI analyses. The effect of kinematic interaction appears to be larger in stiffer soil.  
16

17 b) The effect of kinematic interaction is related to the rotation of the monopile which increases with frequency;  
18 therefore, the effect is largest for the contribution of the second mode to the response of the tower.  
19

20 c) For the same reason stated in b), the kinematic interaction is most important in cases with earthquakes  
21 characterized by medium-to-high frequency content.  
22

23 d) In the practical range of  $L/d$  encountered in OWTs,  $L/d$  does not seem to have any significant role on the seismic  
24 response of OWTs.  
25

26 e) The results presented in this study point to the need for rigorous consideration of kinematic interaction in the  
27 SSI earthquake analyses of OWTs, especially in stiffer soil and in seismic excitations with higher frequencies.  
28  
29

30 **REFERENCES**  
31

32 Andrianopoulos, K.I., Papadimitriou, A.G. Bouckovalas, G.D. 2010. Bounding surface plasticity model for the  
33 seismic liquefaction analysis of geotechnical structures. *Soil Dyn Earthq Eng*; 30(10):895–911.  
34  
35 Álamo, G.M. Aznarez, J.J., Padron, L.A., Martínez-Castro, A.E., Gallego, R. and Maeso, O. 2018. Dynamic  
36 soil-structure interaction in offshore wind turbines on monopiles in layered seabed based on real data. *Ocean*  
37 *Engineering*, 156:14–24.  
38  
39 Auersch, L. 2019. Compliance and damping of piles for wind tower foundation in nonhomogeneous soils by the  
40 finite-element boundary-element method. *Soil Dynamics and Earthquake Engineering*, 120:228-244.  
41  
42 Bayat, M., Andersen, L.V. and Ibsen, L.B. 2016.  $p$ - $y$ - $\dot{y}$  curves for dynamic analysis of offshore wind turbine  
43 monopile foundations. *Soil Dynamics and Earthquake Engineering*, 90:38–51.  
44  
45 Boulanger, R.W., Curras, C.J, Kutter, B.L., Wilson, D.W. and Abghari, A. 1999. Seismic soil-pile-structure  
46 interaction experiments and analyses. *Journal of Geotech. and Geoenviron. Engineering*, 125(9):750-759.  
47  
48 Dezi F, Carbonari S, Morici M. 2016. A numerical model for the dynamic analysis of inclined pile groups.  
49 *Earthquake Engng Struct. Dyn.*, 45:45-68.  
50  
51 Di Laora, R., and Rovithis, E. 2015. Kinematic bending of fixed-head piles in nonhomogeneous soil, *J. Geotech.*  
52 *Geoenviron. Eng.*, 141(4), 04014126.  
53  
54 Di Laora, R., Mylonakis, G. and Mandolini, A. 2017. Size Limitations for Piles in Seismic Regions, *Earthquake*  
55 *Spectra*, 33(2):729-756.  
56  
57 Dafalias Y.F., Manzari, M.T. 2004. Simple plasticity sand model accounting for fabric change effects *J Eng*  
58 *Mech*; 130 (6): 622–634. [https://doi.org/10.1061/\(ASCE\)0733-9399\(2004\)130:6\(622\)](https://doi.org/10.1061/(ASCE)0733-9399(2004)130:6(622))  
59

1 Dobry, R., and O'Rourke, M.J. 1983. Discussion on 'Seismic response of end-bearing piles' by R. Flores-  
2 Berrones and R.V. Whitman. *Journal of the Geotechnical Engineering Division*, 109(5): 778–781.  
3 doi:10.1061/(ASCE)0733-410(1983)109:5(778).  
4

5 Elgamal A, Yang Z, Parra E. 2002. Computational modeling of cyclic mobility and post-liquefaction site  
6 response. *Soil Dyn Earthq Eng*; 22 (4): 259–271. [https://doi.org/10.1016/S0267-7261\(02\)00022-2](https://doi.org/10.1016/S0267-7261(02)00022-2).  
7

8 Esfeh, P.K. and Kaynia, A.M. 2020. Earthquake response of monopiles and caissons for Offshore Wind  
9 Turbines founded in liquefiable soil. *Soil Dynamics and Earthquake Engineering* 136.  
10 <https://doi.org/10.1016/j.soildyn.2020.106213>.  
11

12 Fan, K., Gazetas, G., Kaynia, A., Kausel, E., Ahmad, S. 1991. Kinematic response of single piles and pile  
13 groups. *Journal of Geotechnical Engineering (ASCE)*;117(12): 1860–79.  
14

15 He, R., Kaynia, A.M., Zhang, J., Chen, W. and Guo, Z. 2019. Influence of vertical shear stresses due to pile-soil  
16 interaction on lateral dynamic responses for offshore monopiles. *Marine Structures*. 64:341–359.  
17

18 Jonkman J, Butterfield S, Musial W, Scott G. 2009. Definition of a 5-mw reference wind turbine for offshore  
19 system development, National Renewable Energy Laboratory.  
20

21 Kausel, E., Whitman, R.V., Morray, J.P. and Elsabee, F. 1978. The spring method for embedded foundations.  
22 *Nuclear Engineering and Design*, 48:377–392.  
23

24 Kaynia, A.M. 1982. Dynamic stiffness and seismic response of pile groups. Research Report R82-03, Dept. Civil  
25 Eng., M.I.T. Cambridge, Massachusetts. USA.  
26

27 Kaynia, A.M. and Kausel, E. 1991. Dynamics of piles and pile groups in layered soil media. *Soil Dyn.*  
28 *Earthquake Engrg*, 10(8):386-401.  
29

30 Kaynia, A.M. and Novak, M. 1992. Response of pile foundations to Rayleigh waves and obliquely incident body  
31 waves. *Earthquake Engrg. Struct. Dynamics*, 21(4):303-318.  
32

33 Kaynia, A.M. and Mahzooni, S. 1996. Forces in Pile Foundations under Earthquake Loading. *J. Engrg. Mech.*,  
34 *ASCE*, 122 (1), 46-53.  
35

36 Kaynia, A.M. (2018). Seismic considerations in design of offshore wind turbines. *Soil Dyn. Earthquake Engrg.*  
37 (<https://doi.org/10.1016/j.soildyn.2018.04.038>).  
38

39 Kementzetzidis E., Corciulo S, G. Versteijlen W, Pisanò F. 2019. Geotechnical aspects of offshore wind turbine  
40 dynamics from 3D non-linear soil-structure simulations. *Soil Dyn Earthq Eng*;120:181-199.  
41 <https://doi.org/10.1016/j.soildyn.2019.01.037>.  
42

43 Kjølraug R.A. and Kaynia, A.M. (2015). Vertical earthquake response of megawatt-sized wind turbine with soil-  
44 structure interaction effects. *Earthquake Engineering and Structural Dynamics*. 44:2341-2358.  
45

46 Kourkoulis RS, Lekakakis PC, Gelagoti FM, Kaynia AM. 2014. Suction caisson foundations for offshore wind  
47 turbines subjected to wave and earthquake loading: effect of soil foundation interface. *Géotechnique*  
48 2014;64(3):171 –85. <https://doi.org/10.1680/geot.12.P.179>.  
49

50 Løken, I.B. and Kaynia, A.M. (2019). Effect of foundation type and modelling on dynamic response and fatigue  
51 of offshore wind turbines. *Wind Energy*. 2019;22:1667–1683 (<https://doi.org/10.1002/we.2394>).  
52

53 Manzari M.T, Dafalias Y.F. 1997. A critical state two-surface plasticity model for sands. *Géotechnique*  
54 1997;47(2):255–272. <https://doi.org/10.1680/geot.1997.47.2.255>.  
55

56 Maiorano, R.M.S., de Sanctis, L., Aversa, S. and Mandolini, A. 2009. Kinematic response analysis of piled  
57 foundations under seismic excitation. *Can. Geotech. J.* 46: 571–584 (doi:10.1139/T09-004).  
58

59 Markou, A.A. and Kaynia, A.M. 2018. Nonlinear soil-pile interaction for offshore wind turbines. *Wind Energy*,  
60 21:558–574.

1  
2 Miura, K., Kaynia, A.M., Masuda, K., Kitamura, E. and Seto, Y. (1994). Dynamic behaviour of pile foundations  
3 in homogeneous and nonhomogeneous media. *Earthquake Engrg. Struct. Dynamics*, 23(2):183-192.  
4  
5 Mylonakis, G., Nikolaou, A. and Gazetas, G. (1997). Soil-Pile-Bridge Seismic Interaction: Kinematic and  
6 Inertial Effects. Part I: Soft Soil. *Earthquake Engineering & Structural Dynamics*, 26(3): 337-359.  
7  
8 Mylonakis, G. 2001. Simplified model for seismic pile bending at soil layer interfaces. *Soils and Foundations*,  
9 41(4): 47–58.  
10  
11 Nikolaou, A.S., Mylonakis, G., Gazetas, G., and Tazoh, T. 2001. Kinematic pile bending during earthquakes  
12 analysis and field measurements. *Geotechnique*, 51(5): 425–440. doi:10.1680/geot.51.5.425.39973.  
13  
14 Padrón L.A., Aznárez J.J. and Maeso, O. (2008). Dynamic analysis of piled foundations in stratified soils by a  
15 BEM-FEM model. *Soil Dyn Earthq Eng.*, 28:333–346.  
16  
17 Pender, M. (1993). Aseismic pile foundation design analysis. *Bulletin of the New Zealand National Society for*  
18 *Earthquake Engineering*; 26(1):49-160.  
19  
20 Seed, H.B. and Idriss, I.M. 1970. Soil moduli and damping factors for dynamic response analyses. Report EERC  
21 70-10, EERC, Univ. of California, Berkeley. USA.  
22  
23 Shadlou M., Bhattacharya, S. (2016). Dynamic stiffness of monopiles supporting offshore wind turbine  
24 generators. *Soil Dyn Earthq Eng.* 88:15-32.  
25  
26 Varun, V., Assimaki, D., and Shafieezadeh, A. 2013. Soil-pile-structure interaction simulations in liquefiable  
27 soils via dynamic macroelements: Formulation and validation, *Soil Dynamics and Earthquake Engineering*  
28 47:92–107.  
29  
30 Waas, G. and Hartmann, H.G. 1984. Seismic analysis of pile foundations including pile-soil-pile interaction.  
31 *Proc. 8th World Conf. Earthquake Engrg, San Francisco, California*,5:55-62.  
32